Characteristics of post-impregnated SBA-15 with 12-Tungstophosphoric acid and its correlation with catalytic activity in selective esterification of glycerol to monolaurate

P Y Hoo[1], **A Z Abdullah**[2]
School of Chemical Engineering, Universiti Sains Malaysia, Engineering Campus, Seri Ampangan, Nibong Tebal, Pulau Pinang, Malaysia.

E-mail: [1]arthur.py.hoo@gmail.com, [2]chzuhairi@usm.my

Abstract. Selective esterification of glycerol and lauric acid to monolaurin was conducted using 12-tungstophosphoric acid (HPW) incorporated SBA-15 as catalyst. They were synthesized with HPW loadings of 10–40 wt. % via post impregnation and characterized in terms of surficial and structural characteristic, acidity and morphology. Relatively high lauric acid conversion (up to 95 %) and monolaurin yield (53 %) were observed while the activity was successfully correlated to the material behaviours, i.e. highly acidic active acid sites within highly uniformed mesopores. The effects of different reaction parameters including reactant ratio (1:1-5:1), catalyst loading (1-5 wt. %) and length of fatty acid were also elucidated. Reduced fatty acid conversion was observed when longer fatty acids were used, thus further strengthen the idea of size selectivity effect provided by the synthesized catalysts.

1. Introduction

The global blooming biodiesel production in recent years has resulted in the corresponding increase in glycerol production [1]. In fact, glycerol is formed at a rate of 10wt% of the total biodiesel synthesized [2]. The situation is made worse with further glycerol contribution from oleochemical and soap making industries [3], ultimately resulting in global glycerol price slump due to oversupply [4]. Thus, conversions of glycerol into other value-added chemicals such as monoglycerides are highly encouraged. Certainly, that was never the sole solution to the matter, however, we see the potential of converting waste (glycerol) to gold (monoglyceride as food addictive). As such, the development of heterogeneous catalysis system for such reaction is worth investigation with its own research merit. Traditionally, the monoglyceride was commercially produced via esterification of glycerol with fatty acids at low temperature (90–120℃) using strong homogeneous acids [5]. Though considerably high conversion was achieved, no control whatsoever towards the monoglyceride selectivity was identified. Consequently, extensive purification processes and thus additional costs are needed to enrich the final product and the separation and recycle of homogeneous catalysts.

With such motivation, the development of high-performance heterogeneous catalyst focus on selective monolaurate synthesis was attempted in this study. The exploitation of Keggin-type 12-tungstophosphoric acid (HPW) superacid supported on mesoporous SBA-15 could potentially improve glycerol conversion rate, at the same time provide high selectivity solely towards monolaurate. Our

[1]To whom any correspondence should be addressed

previous study suggested directly synthesized HPW supported SBA-15 could potentially be beneficial to such reaction [6]. However, trapped (and hence inactive) HPW acid sites within the hydrolysed SBA-15 walls, the agglomeration of HPW crystals on the external surfaces and pore deformation at high HPW loading have compromised the catalyst performance. Thus, in this study, we investigated HPW supported SBA-15 via wetness incipient method to minimize the structural modification of parent SBA-15. As such, we would be able to investigate if any improvement on the catalysts could be achieved from both characterization and catalytic performance point of view.

2. Experimental methods

2.1. Synthesis of SBA-15 support and HPW post impregnated SBA-15

The typical SBA-15 support was synthesized as reported in the literature [7]. HPW was incorporated into SBA-15 at 10 to 40wt% loading via incipient wetness impregnation method. The appropriate amount of post synthesized SBA-15 was wetted with deionized water (2.5 ml/g SBA-15). On the other hand, an appropriate amount of HPW was dissolved in deionized water (1 ml/g SBA-15). Under rapid stirring, HPW solution was added dropwise into the wetted SBA-15. The mixture was then dried at 60℃ for 12 hours and followed by another 12 hours at 100℃. The catalysts were then named X wt. %-HPW/IM, with X = 10, 20, 30, 40.

2.2. Characterization of synthesized support and catalysts

Morphology characterizations were done via liquid Nitrogen (N_2) desorption using Quanta-Chrome Autosorb 1C surface analyser and Philips CM12 transmission electron microscope (TEM). The structural properties including available functional groups were investigated with the help of Shimadzu IRPrestige-21 Fourier Transformed Infrared (FTIR) (KBr pellet method). All catalysts were pre-treated in Helium (He) gas and exposed to ammonia (NH_3) mixture (15% NH_3, 85% He) before subject to desorption from 100℃ to 750℃ with ramping of 10℃/min to obtain the acidity profiles via ammonia temperature programmed desorption (NH_3-TPD).

2.3. Catalytic performance assessment

All synthesized catalysts were subjected to the measurement of their respective catalytic performance. A batch reactor consists of a three-necked flask was connected to a temperature probe with temperature controller, magnetic stirrer and vacuum pump. The reactor was used for selective esterification of glycerol with lauric acid with the presence of the catalyst at designated reaction temperature, reactant ratio and catalysts loadings. Samples were collected at appropriate period of times and were analysed using Agilent Technologies 7890A GC equipped with a CP-Sil 5CB (15 m x 0.32 mm x 0.1 mm) column. Lauric acid conversion and the selectivity for monolaurate, dilaurate and trilaurate were calculated accordingly [8].

3. Results and discussions

3.1. Characterizations of HPW post impregnated SBA-15

In order to understand the surficial properties of the synthesized catalyst, N_2 adsorption-desorption test was performed on all the synthesized materials. Table 1 showed the result from the surface analyses. It was evidenced that even after impregnation of HPW (up to 40 wt%), mesoporosity could be observed (55 – 59 Å) with high surface areas (323 – 600 m^2/g). The decrease in surface areas with increasing HPW loading provided indirect evidence of successful impregnation of HPW onto the SBA-15 support due to deposition of HPW anions on the inner pore walls [9]. From Figure 1, Type IV N_2 absorption-desorption isotherms were shown by all catalysts, proving the retained mesoporosity of these catalysts [10]. While on Figure 2, it was obvious that uniformed pores were formed in the virgin SBA-15, though 2 major peaks could be found (around 40 Å and 60 Å). Interestingly, with the

impregnation of HPW, both peaks intensities decreased, suggesting successful impregnation of HPW on the inner pores surfaces. Such finding was in agreement with the observations found in Table 1.

Table 1. Summary of surface characteristics of synthesized catalysts.

Catalysts	Total surface area (m^2/g)[a]	Micropores area (m^2/g)[b]	External surface area (m^2/g)[b]	Micropores volume (cm^3/g)[b]	Total pore volume (cm^3/g)[c]	Average pore size (Å)[c]
SBA-15	640	169	471	0.078	0.65	61
10wt%-HPW/IM	600	137	464	0.070	0.62	59
20wt%-HPW/IM	552	119	433	0.061	0.61	58
30wt%-HPW/IM	368	102	267	0.048	0.43	55
40wt%-HPW/IM	323	89	235	0.045	0.40	58

[a]BET desorption method; [b]t-plot method; [c]BJH desorption method

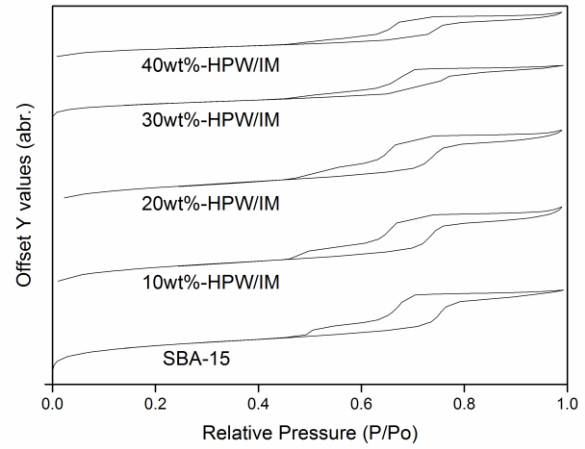

Figure 1. Nitrogen adsorption-desorption isotherms of SBA-15 and HPW post impregnated catalysts of 10wt% to 40wt% loadings.

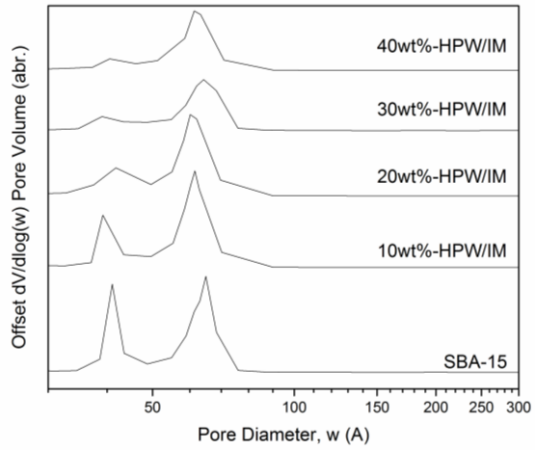

Figure 2. BJH pore size distribution of SBA-15 and HPW post impregnated catalysts of 10wt% to 40wt% loadings.

TEM images of all synthesized catalysts were shown in Figure 3. These TEM images clearly showed long, highly ordered mesoporous hexagonal channels of the famous SBA-15 remained unchanged even up to 40wt% HPW loading. It was also clear that the HPW anions were successfully incorporated into the inner pores of SBA-15 (narrowing of SBA-15 channels), yet without pore blockage (high surface areas remained) unlike the direct synthesized HPW support SBA-15 in our previous study [6]. Via post impregnation method, SBA-15 mesopores networks were stable prior to the addition of HPW anions. As such, any possible deposition of HPW anions could only occurred on the external surfaces or inner pore surfaces of SBA-15 supports, unlike those direct synthesized ones. Furthermore, high solubility of Keggin HPW anions and high mobility of water into the SBA-15 inner pores reduced the agglomeration of HPW that would cause pore deformation. As a conclusion, highly uniformed and long hexagonal mesopores have been successfully synthesized and retained in all catalysts even after impregnation of HPW.

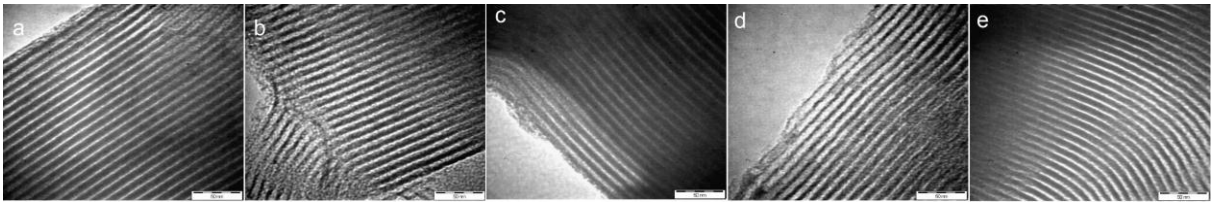

Figure 3. TEM images of a) SBA-15, b) 10wt%-HPW/IM, c) 20wt%-HPW/IM, d) 30wt%-HPW/IM and e) 40wt%-HPW/IM.

The characteristic bands of Si-O-Si condensed silica network of SBA-15 including symmetric (802 cm^{-1}), asymmetric (1220 – 1076 cm^{-1}) and bending vibration of Si-O-Si (459 cm^{-1}) were identified in Figure 4 [9]. Such observation confirmed the successful synthesis of the hydrolysed SBA-15 silica walls. Characteristic bands of Keggin type HPW are also found at the 800 – 1200 cm^{-1} wavenumber region. Interestingly, the increased intensities of Si-OH attributed bands at 3453 cm^{-1} suggested possible interaction between Si-OH with other polar molecules [11]. However, pre-treatment was performed on all the samples to remove physisorbed water, thus the effect of physisorbed water molecules should be of minimal. Such band also showed changes with increasing HPW content supported on SBA-15. It is understood that polyoxoanions (PW^{3-}) could interact with its surrounding via its terminal asymmetric oxygen ($W=O_d$), corner shared asymmetric oxygen ($W-O_b-W$) and/or edge shared oxygen ($W-O_c-W$) [12]. Based on the understanding that no exchange or sharing of electron has occurred, no ionic or covalent bonding would be formed between the support and acid. However, the interfacial Keggin structured PW^{3-} is electron rich [13]. We deduce that such characteristic can potentially act as electron donors to form hydrogen bond with silanol groups of SBA-15.

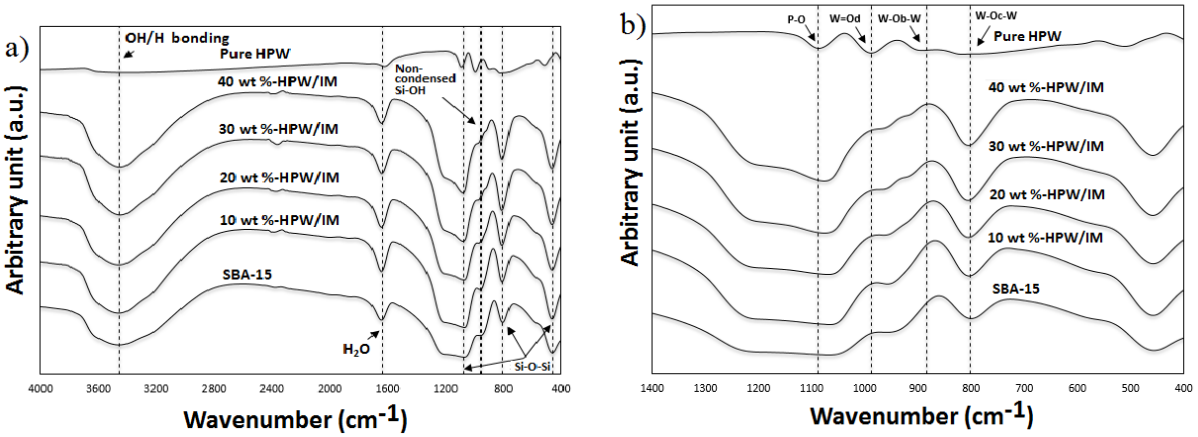

Figure 4. FTIR of all synthesized catalysts at a) 400 – 4000 cm^{-1} and b) 400 – 1400 cm^{-1} wavenumber

The characterization of an acidic catalyst would not be completed without elucidating its acidity profile. Acid strengths classification of these developed catalysts were tabulated in Table 2 [14-16]. As contrast to other reports, the total acidity profiles showed "reverse" volcano shape distribution with increasing acid loadings [17,18]. Thought similar trend was reported [19], we concluded that partial agglomeration of HPW crystal on external surfaces at high HPW loading might have occurred. Nevertheless, comparatively strong acidity profiles (medium and strong acid sites) possessed by 40wt%-HPW/IM was found to be the most beneficial to our study as it was reported that strong Brønsted acid sites were of utmost importance in esterification process [16].

Table 2. Acidity characterization of post impregnated catalysts at different HPW loadings.

Catalysts	Area Under Graph								Relative Acidity
	Weak Acid[a]	%	Medium Acid[b]	%	Strong Acid[c]	%	Total Area	Specific Area	
10wt%-HPW/IM	3.35	66	1.40	28	0.30	6	5	101	2.3
20wt%-HPW/IM	0.81	39	0.94	46	0.31	15	2	40	1.0
30wt%-HPW/IM	2.43	64	1.18	31	0.17	5	4	75	1.4
40wt%-HPW/IM	1.77	8	14.6	70	4.62	22	21	397	8.8

[a] Within temperature range of 100 – 250 ^{0}C [14,15]; [b] Within temperature range of 250 – 450 ^{0}C [15,16];
[c] Within temperature range of 450 – 500 ^{0}C [15,16]

3.2. Catalytic performances of HPW post impregnated SBA-15

The catalytic performances of post impregnated HPW/SBA-15 using wetness incipient method were studied with selective esterification of glycerol with lauric acid producing monolaurate. Parameters included HPW loadings (Figure 5), type of long chain fatty acid (Figure 6), catalyst weight (Figure 7) and glycerol to lauric acid ratio (Figure 8) were studied. From Figure 6, it was observed that while all post impregnated HPW/SBA-15 showed lower conversion compared to pure homogeneous HPW, monolaurate yield of post impregnated HPW/SBA-15 at the end of reaction rivalled to that of pure homogeneous HPW. It was understood that homogeneous HPW could not provide any shape or size control to the reaction. Thus, mono, di and trilaurate might be formed at any given time [7]. Due to active acid sites situated within mesopores, the formation of products could only occur within these pores. Thus, the formation of di and trilaurate are discouraged due to steric hindrance effect within these pores with acid sites. Ultimately, the objective of limiting reaction to form monolaurate was achieved. The effect of steric hindrance was magnified in Figure 6 whereby shorter (capric acid) and longer (myristic and palmitic) fatty acid were used as reactant. Shorter fatty acids were found to have much higher conversion as compared to longer fatty acids. As such, the size constraint effect contributed by the synthesized catalyst was concluded to be effective and significance towards the final products formation.

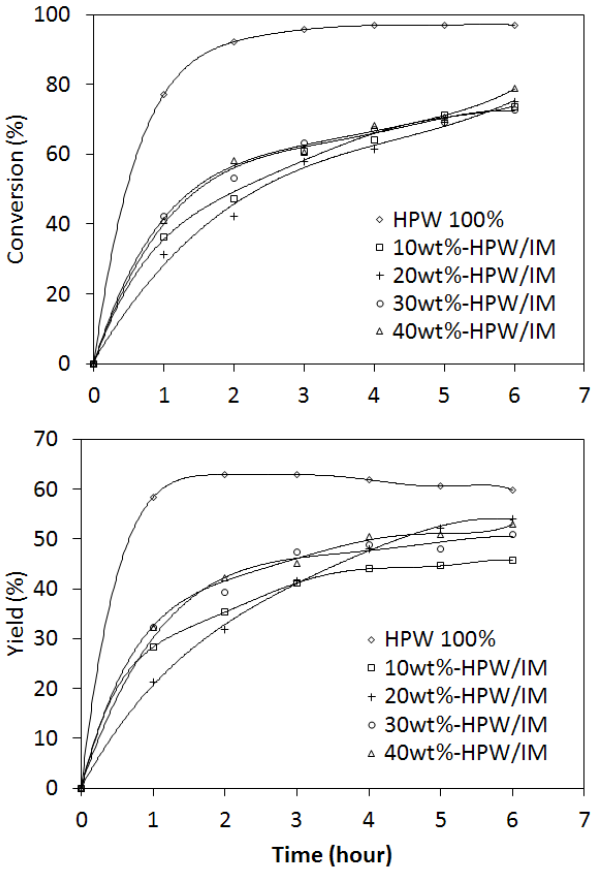

Figure 5. (Top) Lauric acid conversion profiles and (Bottom) monolaurate yield profiles with different HPW loadings.

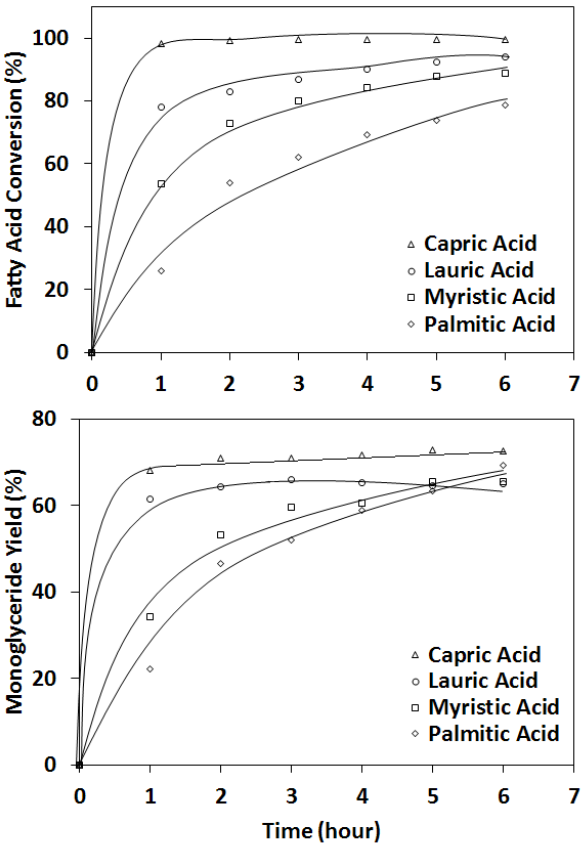

Figure 6. (Top) Long chain fatty acid conversion profiles and (Bottom) their respective monoglycerides yield profiles.

As the most potential catalyst, 40wt%-HPW/IM was chosen to further elucidate the effect of varying reactants ratio and catalyst weight as shown in Figure 7 and 8. When more catalysts were used, higher conversions were achieved. However, the selectivity of monolaurate suffered due to the increased available acid sites encouraged further esterification of monolaurate to di or trilaurate. Although the similar conversions were found when different reactant ratio used, the monolaurate yield was found to be highest at higher ratio. It was understood that esterification of glycerol with fatty acid is reversible, continuous reaction [20]. Dilution of monolaurate by glycerol and Le Chatelier's Principle dictates the formation of monolaurate rather than di or trilaurate.

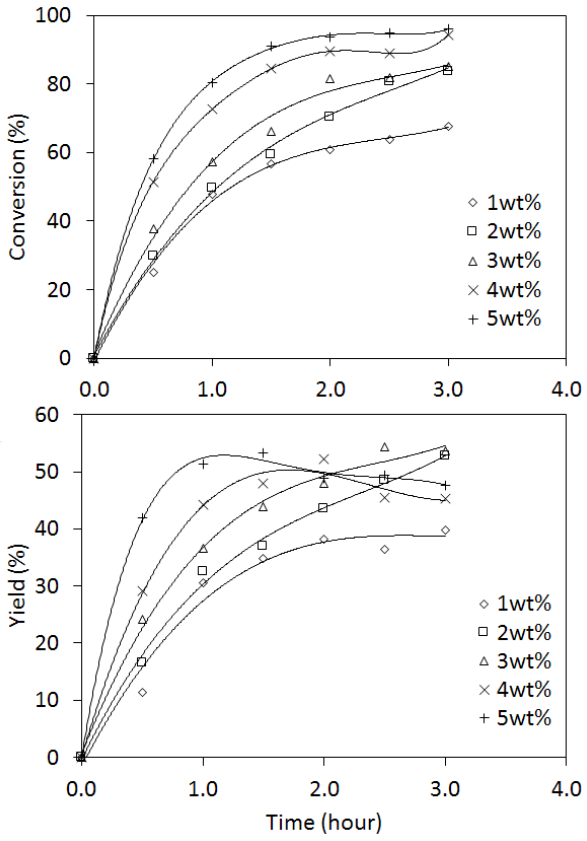

Figure 7. (Top) Lauric acid conversion profiles and (Bottom) monolaurate yield profiles at different catalysts weights used.

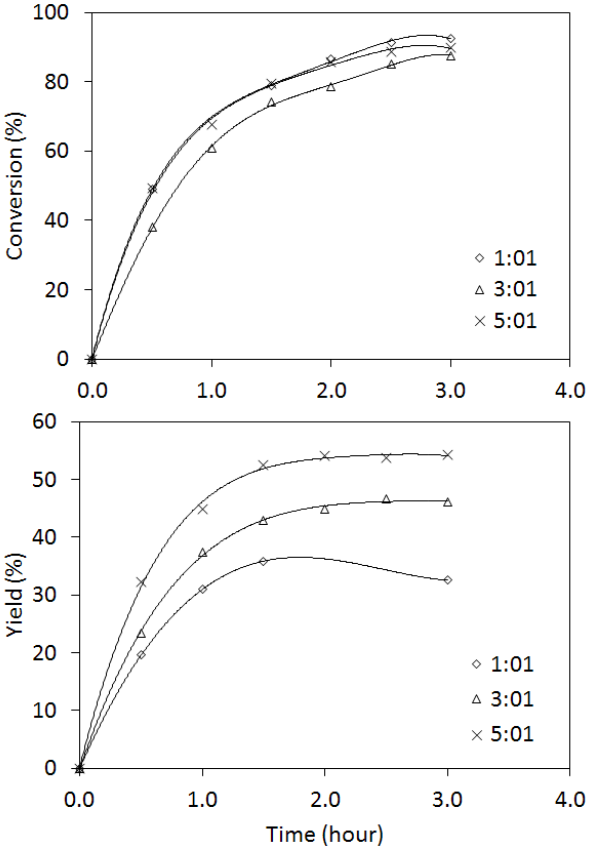

Figure 8. (Top) Lauric acid conversion profiles and (Bottom) monolaurate yield profiles at different glycerol to lauric acid ratio.

4. Conclusion

Post impregnated HPW on SBA-15 with different loadings were synthesized and the surface morphologies, pore structures and elemental analysis were characterized. When compared to directly synthesized HPW on SBA-15 catalysts in our previous study, only low degree of disruption towards the morphologies and pore structures of the support were found, as suggested by both surface characterization and TEM images. At the same time, strong acid sites could be identified from all post impregnated catalysts, especially 40wt%-HPW/IM which possessed the highest acidity from NH_3-TPD analysis. The NH_3-TPD also showed that highly acidic acid sites were accessible situated within the mesopores that would be beneficial to the selectiveness of the catalysts. These developed catalysts showed further improvement on the conversion and monolaurate yield in the selective esterification as tested in this study. Perhaps the most important finding would be the elucidation of the size selectivity of the developed catalysts, as demonstrated by the higher catalytic performance when shorter fatty acid were used. Such result further strengthen the claim whereby the highly active acid sites of these developed catalysts were situated within the mesopores, thus allowing size selectivity to be possible in the tested reaction.

5. References

[1] U.S. Energy Information Administration, E. International Energy Statistics: World Biodiesel Production. 2014 Available online: http://goo.gl/d3NP1F
[2] Rahmat N., Abdullah A Z and Mohamed A R 2010 *Renewable Sustainable Energy Rev*. **14** 987
[3] Bagheri S, Julkapli N M and Yehye W A 2015 *Renewable Sustainable Energy Rev.* **41** 113
[4] Quispe C A, Coronado C J and Carvalho Jr J 2013 *Renewable Sustainable Energy Rev*. **27** 475

[5] Pagliaro M, Ciriminna R, Kimura H, Rossi M and Della Pina C 2007 *Angew. Chem., Int. Ed.* **46** 4434
[6] Hoo P Y and Abdullah A Z 2014 *Chem. Eng. J*. **250** 274
[7] Hermida L, Abdullah A Z and Mohamed A R 2010 *J. Appl. Sci.***10** 3199
[8] Pouilloux Y, Abro S, Vanhove C and Barrault J 1999 *J. Mol. Catal. A: Chem*. **149** 243
[9] Brahmkhatri V and Patel A 2011 *Appl. Catal., A*. **403** 161
[10] Pierotti R and Rouquerol J 1985 *Pure Appl. Chem.* **57** 603
[11] Wang X, Lin K S, Chan J C and Cheng S 2005 *J. Phys. Chem. B,* **109** 1763
[12] Uskoković-Marković S, Colomban P, Mioč U and Todorović M 2007 *Mater. Sci. Forum* **555** 201
[13] Rao G R and Rajkumar T 2008 *J. Colloid Interface Sci.* **324** 134
[14] Molnár Á, Keresszegi C and Török B 1999 *Appl. Catal. A.* **189** 217
[15] Yang L, Qi Y, Yuan X, Shen J and Kim J 2005 *J. Mol. Catal. A: Chem.* **229** 199
[16] Sakthivel R and Kemnitz E 2008 *Indian J. Chem. Technol.* **15** 36
[17] Balaraju M, Nikhitha P, Jagadeeswaraiah K, Srilatha K, Sai P P S and Lingaiah N 2010 *Fuel Process. Technol.* **91** 249
[18] Zhang J, Kanno M, Wang Y, Nishii H, Miura Y and Kamiya Y 2011 *J. Phys. Chem. C*, **115** 14762
[19] Dong B B, Zhang B B, Wu H Y, Chen X, Zhang K and Zheng X C 2013 *Mater. Res. Bull.* **48** 2491
[20] Macierzanka A and Szeląg H 2004 *Ind. Eng. Chem. Res*. **43** 7744

Acknowledgments
The authors thank the Universiti Sains Malaysia (USM) and School of Chemical Engineering for all the financial and technical supports. A Research University grant (814181) and Transdisciplinary Research Grant Scheme (6762001) from Universiti Sains Malaysia are also gratefully acknowledged.